Insights into the interplay between molecular structure and diffusional motion in 1-alkyl-3-methylimidazolium ionic liquids: a combined PFG NMR and X-ray scattering study

Manuel Maréchal, A. Martinelli, Å. Östlund, J. Cambedouzou

Insights into the interplay between molecular structure and diffusional properties in 1-alkyl-3-methylimidazolium ionic liquids. A combined PFG NMR and X-ray scattering study.

A. Martinelli,[a]* M. Maréchal[b]*, Å. Östlund[a], J. Cambedouzou[c]

Received Xth XXXXXXXXXX 2011, Accepted Xth XXXXXXXXX 2011

First published on the web Xth XXXXXXXXXX 2011

DOI: 10.1039/b000000x

We report on how the local structure and transport properties change on increased alkyl chain length in 1-alkyl-3-methylimidazolium cation ionic liquids. This study has been performed by combining pulse field gradient (PFG) nuclear magnetic resonance (NMR) spectroscopy and Small Angle X-ray Scattering (SAXS) experiments. The cationic side chain length varies from ethyl (n=2) to hexadodecyl (n=16), while the anion is always bis(trifluoromethanesulfonyl)imide (TFSI). We find that the self-diffusivity of the individual ionic species is correlated to the local structure in the corresponding ionic liquid, namely the nano-segregation into polar and non-polar domains. In agreement with previous results, we observe that for relatively short alkyl chains the cations diffuse faster than the anions; however we also note that this difference becomes less evident for longer alkyl chains and a cross-over is identified at n≈8 with the anions diffusing faster than the cations. Our results indicate that this controversial behavior can be rationalized in terms of different type of cation–cation and anion–anion orderings, as revealed by a detailed analysis of the correlation lengths and their dispersion curves obtained from SAXS data. We also discuss the validity of the Stokes-Einstein relation in these ionic liquids and the evolution of the extrapolated cationic radius that we find to depend non strictly linearly on *n*, in agreement with the cation-cation correlation lenghts.

Keywords: Ionic Liquids, Nanoscale Ordering, Ionic Transport, PFG NMR, Small Angle X-ray Scattering.

1 Introduction

Ionic liquids, also known as low-temperature molten salts, combine a set of properties like non-flammability, non-volatility, wide electrochemical windows, high ionic density (only ions) and intrinsically high ionic conductivity; they also behave as good solvents for various chemical and electrochemical processes. Because ionic liquids can be synthesized in a wide variety of cation-anion structural combinations, they are also known as *designer solvents*.[1] These attributes make ionic liquids interesting materials for diverse applications, especially where they can be used to drive environmentally benign chemical reactions.[2] In particular, the interest in ionic liquids as electrolytes for fuel cells and Li-ion batteries (two examples of green energy conversion devices of the future) has boosted during the last decades.[3]

Compared to conventional salts or organic solvents, ionic liquids show remarkably low melting temperatures, which is mainly due to the packing frustration in the solid as a consequence of the symmetry breaking structure of the cations.[4] However, other factors like charge delocalization, bulkiness and conformation of the anion also contribute.* Not only the phase behavior is strongly affected by the molecular structure of the constituting ions, but also other macroscopic properties like miscibility, viscosity, conductivity, diffusivity, etc. Understanding the structure-property relationship in ionic liquids is of high interest and inherently related to the strive for tailor-made materials with specific applications. Structural features become particularly interesting if ionic liquids are used to orient reactants, thereby inducing reaction selectivity, or act as templates in the synthesis of mesoporous materials.[6]

Another peculiarity with ionic liquids is that even in the liquid state they can display structural ordering, as in the case of alkyl-imidazolium[8,9] and alkyl-ammonium[7] cations. Small angle X-ray and neutron scattering (SAXS and SANS) data have shown that provided sufficiently long alkyl chains, the

* *Corresponding authors. E-mail: anna.martinelli@chalmers.se or manuel.marechal@lepmi.grenoble-inp.fr.*

[a] *Applied Surface Chemistry, Chemical and Biological Engineering, Chalmers University of Technology, Gothenburg, Sweden.*

[b] *LEPMI UMR 5279 (CNRS-Université de Grenoble), Saint Martin d'Hères, France.*

[c] *ICSM UMR 5257 (CEA-CNRS-UM2-ENSCM), Bagnols sur Cèze, France*

* For example by substituting Na^+ by the bulkier and asymmetric cation 1-butyl-3-methylimidazolium ($BMIM^+$) the melting temperature of the corresponding salt decreases from 800 °C (NaCl) to 70 °C ($BMIM^+Cl^-$), and further to -4 °C ($BMIM^+TFSI^-$) when substituting Cl^- with the charge delocalized TFSI anion. Also, in ionic liquids of the $TFSI^-$ a combination of the two conformational forms C_1 (*cisoid*) and C_2 (*transoid*) are normally found in the melted phase, while C_2 is typical of the solid state.[5]

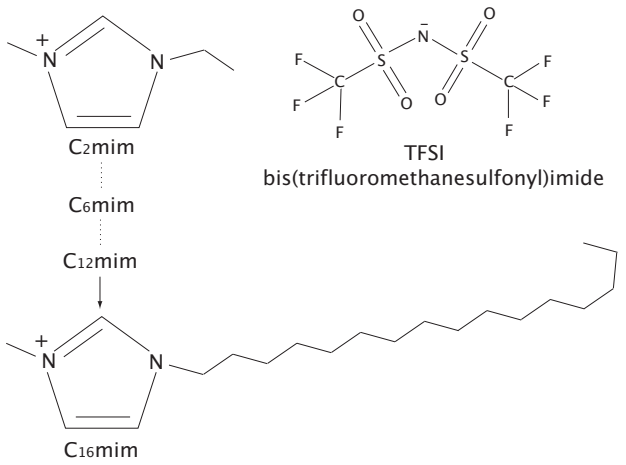

Fig. 1 Molecular structure of the ingoing ions in the investigated ionic liquids. The imidazolium cations have an alkyl side chain whose length varies from 2 to 16 carbon atoms (C_nH_{2n+1} where n=2, 4, 6, 8, 10, 12 and 16). The bis(trifluoromethanesulfonyl)imide anion, also known as $TFSI^-$, is also shown.

cations tend to self-aggregate resulting in polar and non-polar domains of the nanometer size. A model similar to the structuring observed in linear alcohols has been proposed,[10,11] although the inter-digitation of the hydrophobic chains seems to be limited in ionic liquids.

Furthermore, this nano-segregation has been reported for diverse anions (Cl^-, $BF_4{}^-$, $PF_6{}^-$ and $TFSI^-$) where the size of the nano-domains is believed to scale linearly with the length of the alkyl chain (the length being defined by n in $-C_nH_{2n+1}$, see Figure 1). This linearity, however, has so far mainly been discussed for chains where n is smaller than, or equal to, 8. The length of the alkyl chain on the cation does not only result in nano-segregation but can also indirectly affect other properties. For instance, both viscosity and ionic association increase with n, as a result of stronger van der Waals interactions.[12] For applications where the mobility of ionic species is functional,† understanding the relationship between structure and transport properties becomes crucial.

In some ionic liquids, cations and anions have shown distinct diffusive behaviors. Tsuzuki *et al.*[13] have investigated a series of 1-alkyl-3-methylimidazolium ionic liquids in the range $2 \leq n \leq 8$ reporting higher self-diffusion coefficient for the cation, compared to the anion, from both molecular dynamic (MD) simulations and diffusion NMR experiments. Although calculations systematically underestimated the experimentally recorded self-diffusion constants, both trends showed decreasing values for increasing alkyl chain lengths, consistently with lower measured conductivities.[12] MD simulations were also specifically employed on the ionic liquid 1-butyl-3-methyl-imidazoliumTFSI to further elucidate on this controversial behavior.[14‡] The authors found anisotropies in the cation displacement, with a preferential motion parallel to the imidazolium ring and along the alkyl chain axis. More specifically, the diffusing behavior was rationalized by the non-uniform way in which anions surround the cation, leaving a region near the alkyl chain less populated with counterions. Yet, it is not completely clear what structural features may govern this dynamical controversy.

In this paper, aiming to better understand the correlation between the transport properties and the local structure in imidazolium-based ionis liquids, we combine a detailed analysis of diffusion NMR and SAXS data. With respect to previous studies we contribute with a larger structural variation including cations with alkyl chain lengths that range from ethyl (*n=2*) to hexadecyl (*n=16*). This larger series allows discussing the true linearity of the cation-cation correlation lengths and the structural models proposed so far. We also add some new value to previously reported SAXS (and WAXS) studies by including an analysis of the dispersion curves associated to the correlation lengths. In fact, beyond giving evidence of a certain ordering (through indexing of diffraction peaks) SAXS data can also provide information on the nature of cation-cation, anion-anion and cation-anion ordering, which we elucidate in this work.

2 Experimental

2.1 Materials

The 1-alkyl-3-methylimidazolium ionic liquids of the bis(trifluoromethanesulfonyl)imide anion, TFSI, and alkyl chain $-C_nH_{2n+1}$ with n varying from 2 to 16 were purchased from Iolitec. All ionic liquids were immediately transferred and stored in an Ar-gas filled glove box. The samples were also prepared and sealed in the glove box.

2.2 Conductivity measurements

The impedance spectroscopy measurements were carried out using a Materials Mates 7260 frequency response analyzer. The spectra were recorded between 10 Hz and 10 MHz with the temperature controlled at ± 0.1 °C. The symmetrical cell with platinum-plated square working electrodes was calibrated for the conductivity and temperature ranges investigated to prevent artifacts. The data were fitted with phenomenological models after correcting from the set-up impedance.

† In e.g. fuel cells or Li-ion batteries.

‡ The reader should note that the self-diffusion coefficient of the cation is not always higher than that of the anion. In BPTFSI, for instance, the cation diffuses faster than the anion, but not in $BPBF_4$ (where BP is butylpyridinium).[15]

2.3 Diffusion NMR experiments

Diffusion NMR experiments were performed on a Bruker Avance 600 spectrometer. Samples were kept in NMR tubes and equilibrated for at least 20 minutes at the desired temperature before starting any measurement. The self-diffusion coefficient, D, was estimated by fitting the echo signal decay. The normalized signal attenuation depends on the strength, g, and length, δ, of the gradient pulses, the time between the gradients, Δ (diffusion time), and the self-diffusion coefficient, D, of the molecules related to the normalized signal intensity, I/I_0, as described by the Stejskal-Tanner equation $I/I_0=1/2\cdot e^{-(\gamma^2 g^2 D\delta^2)(\Delta-\delta/3)}$.[16] In order to verify that convection within the sample tube did not influence the measurements, we repeated PFG NMR experiments for diverse sets of Δ-δ values, whereby the self-diffusion coefficients were found not to depend on Δ. Furthermore, to ensure the consistency of reported D values we employed two different pulse sequences, namely the stimulated echo (Ste) and the double stimulated echo (DSte) pulse sequences. The calibration of the magnetic field gradient was performed at 25 °C using D_2O as reference,[17] while the consistency of ^1H and ^{19}F diffusion experiments was controlled on the reference sample trifluoroethanol (CF_3CH_2OH) whose molecular structure contains both F and H atoms.

2.4 X-ray Scattering

Small- and Wide-Angle X-ray scattering (SAXS and WAXS) measurements were performed using a Xenocs setup equipped with a Mo GENIX anode over the large q-range 0.23–30 nm^{-1}. The K_α radiation (λ = 0.071 nm) was selected and multilayered curved mirrors were used to focus the beam at infinity. The size of the beam at the sample position (0.8 x 0.8 mm^2) was defined by two sets of scatterless FORVIS slits. The scattered beam was recorded using a large online scanner detector (345 mm in diameter from MAR Research) positioned 742 mm from the sample. Sample and empty cell transmissions were determined using an offline pin diode that can be inserted downstream from the sample. Quartz capillaries (2.5 mm in diameter with a wall thickness of 0.01 mm) from Hilgenberg were used as sample containers. FIT2D was used to treat the data and the standard procedure for background subtraction (empty cell and detector noise) and intensity normalization was applied using a 2.36 mm thick low density polyethylene film from Goodfellow. The scattered intensities are expressed as a function of the scattering vector q, where $q = (4\pi/\lambda)\cdot\sin(\theta/2)$, λ is the wavelength of the incident beam, and θ the scattering angle. The standard silver behenate was used for the q-range calibration. The experimental resolution was $\Delta q/q = 0.05$.

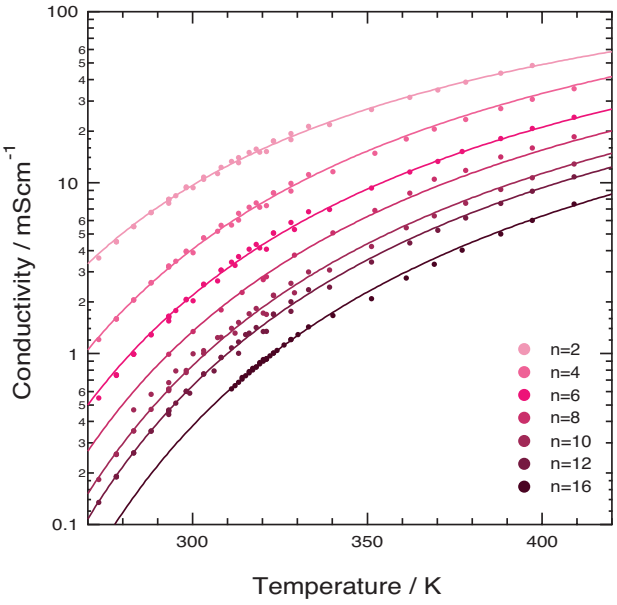

Fig. 2 Temperature dependence of the ionic conductivity for the 1-alkyl-3-methylimidazolium TFSI ionic liquid series; n increases from top to bottom. These experimental data have been fitted by the Vogel-Tamman-Fulcher (VTF) equation (solid lines).

3 Results and discussion

3.1 Ionic conductivity

Figure 2 shows the ionic conductivity for the whole series of ionic liquids as a function of temperature. This plot evidences that the ionic conductivity increases with temperature for all alkyl chain lengths, as expected and in agreement with previous studies.[12] Still in agreement with other results, we find that these conductivity data do not follow an Arrhenius behavior but are best fit with the Vogel-Tamman-Fulcher (VTF) equation, $\sigma = \sigma_0\cdot e^{-B/(T-T_0)}$, where B is a parameter closely related to the fragility of the material (fragility is in fact proportional to T_0/B and is an important property in glass-forming liquids),[18] T_0 is the ideal glass transition temperature and σ_0 is the conductivity at temperatures much larger than T_0. These fitting parameters are summarized in Table 1. After collapsing between n=2 and 4, the fragility monotonically decreases with n, which is associated to the evolution of the structural heterogeneity. Indeed, as n increases, the connectivity between the non-polar domains becomes stronger with a consequent increase of the activation energy (E_a=R·B, where R is the universal gas constant),[19] which is the energy related to an elementary step of the ionic transport. Thus, the growth of the non-polar domain network concomitant with the increase of its connectivity dynamically restricts the polar domain network.

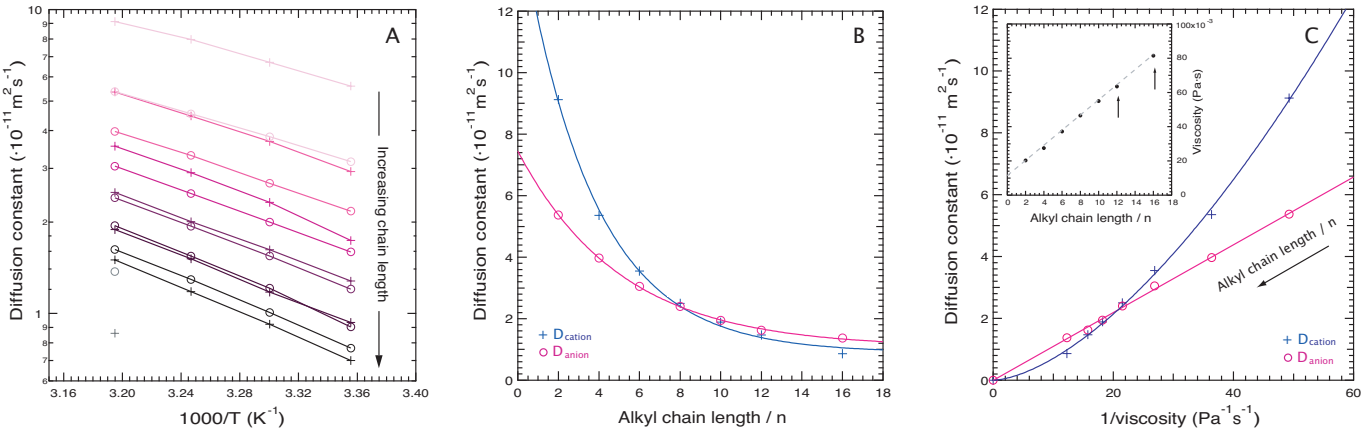

Fig. 3 Self-diffusion coefficients for the cation D_+ (+) and the anion D_- (○) in 1-alkyl-3-methylimidazolium ionic liquids shown in an Arrhenius plot (A), as a function of alkyl chain length, at 40 °C, (B) and as a function of inverse viscosity, at 40 °C, (C). The inset in C shows the dependence of viscosity on alkyl chain length, data reproduced from references 20 and 22.[20,22]

Table 1 VFT fitting parameters for the ionic conductivity data and calculated *'fragility'* values.

n (chain length)	σ_0 [S cm^{-1}]	T_0 [K]	B [K]	*'fragility'* T_0 / B
2	0.6	148.04	626.84	0.23617
4	0.68	148.57	772.14	0.19241
6	0.63	151.14	840.89	0.17974
8	0.59	152.72	886.78	0.17222
10	0.52	148.19	929.24	0.15947
12	0.5	149.4	998.94	0.14956
16	0.47	140.78	1109.8	0.12685

3.2 Self-diffusivity

Figure 3A shows the self-diffusion constants as a function of temperature for both the anion (D_-) and the cation (D_+) for the alkyl chain length varying from n=2 to n=16. These D values are found in the range 0.6–10·10^{-11} m^{2}s^{-1}, in agreement with previously reported data.[13,20] Consistently with the values reported in reference [13][13], we also observe that the diffusion coefficients decrease with the alkyl chain length, *n*.

The self-diffusion coefficients increase with temperature with an apparent linear dependence. In fact an Arrhenius equation of the type $D=D_0 \cdot e^{-Ea/(RT)}$ does not fit the experimental data, which are on the other hand very well described by the Vogel-Tamman-Fulcher equation $D=D_0 \cdot e^{-B/(T-T_0)}$. However, due to the narrow temperature range here investigated,§ and consequently a small number of data points, we do not aim at estimating the parameters D_0, B and T_0 from PFG NMR experiments. Nevertheless, the trend that we observe is in agreement with previous studies on imidazolium ionic liquids, whose diffusion constants investigated for wider temperature intervals manifest the typical VTF dependence.[15]

Figure 3A also evidences that for relatively small chain lengths the cation diffuses faster than the anion. This peculiarity was also observed by Noda *et al.*,[15] who investigated the transport properties in four ionic liquids of the imidazolium and pyridinium cation, associated to either BF_4^- or $TFSI^-$. This behavior had previously been predicted by MD simulations and attributed to the more dynamically heterogeneous environment of the cation with respect to the anion.[13,14] In reference [14][14] it is also argued that the cations have a larger rotational anisotropy than anions, even though this difference rapidly decreases with temperature.

The individual dependence of D_+ and D_- on the side chain length *n* is more clearly displayed in Figure 3B for the representative temperature of 40 °C.¶ This plot evidences the discrepancy between the self-diffusion constants of cations and anions that, however, becomes smaller for longer chain lengths, eventually showing a cross-over at *n*=8. This behavior could have been deduced from the data reported by Tsuzuki *et al.*,[13]‖ although it was not at focus there and also the structural variation limited compared to the present study. The occurrence of this cross-over is here experimentally evidenced for the first time and is extremely interesting in relation to the local structural evolution that it may be correlated to. If a certain structural organization is the reason for D_+ being larger

§ Due to technical limitations of the employed NMR spectrometer.

¶ All imidazolium salts here investigated are liquid at this temperature except the C_1C_{16}TFSI. This ionic liquid was therefore first equilibrated at 70 °C (at which it is melted) and then quickly inserted into the spectrometer for PFG NMR experiments.

‖ See in particular Figure 4 in reference [13][13].

than D_- for short alkyl chains,[14] it is also reasonable that new local structures are the origin of the observed cross-over for longer chains. We have approached this issue by a thorough analysis of experimentally recorded SAXS data, discussed in more detail in section 3.3.

One common way to interpret self-diffusion coefficients is in relation to viscosity through the Stokes-Einstein equation:

$$D = k_B T / c\pi r\eta \quad (1)$$

which is generally valid for classical hydrodynamic systems. In the Stokes-Einstein relation k_B is the Boltzmann's constant, T the temperature, r the hydrodynamic (or Stokes) radius, c the coupling factor (that for ideal hydrodynamic systems is 6 whilst closer to 4 for ionic liquids), and η the macroscopically measured viscosity. Thus, ideally, at constant viscosity and temperature, the self-diffusion should decrease for increasing diffusive radii. An alternative way of representing the Stokes-Einstein relation is the fractional form:

$$D \propto (T/\eta)^{\beta} \quad (2)$$

in which it is assumed that the $k_B/(c\pi \cdot r)$ prefactor is a constant. In equation (2) β takes the value of one for conventional dilute electrolytes, whereas for ionic liquids of the 1-butyl-3-methylimidazolium cation (C_1C_4) investigated so far** β has been found to be in the range 0.92–0.95.[14,21] Hence, classical hydrodynamic considerations may not be strictly valid in all ionic liquids.[14]

In Figure 3C, D_+ and D_- are individually plotted versus inverse viscosity. Note that in this plot n is a variable that increases from the upper-right to the lower-left corner. The viscosity values used to construct this plot are those reported by Tokuda *et al.* in reference [20][20] and extrapolated from reference [22][22] (see inset). The plot in Figure 3C reveals very different behaviors for anions and cations: while D_- increases linearly with $1/\eta$, the dependence of D_+ deviates from linearity. Different cationic and anionic behaviors were also observed by Noda *et al.*,[15] with the cations showing a stronger dependence on $1/\eta$ than the anions.†† The authors also comment on the mismatch between the slopes derived from the Stokes-Einstein relation and the real size of the diffusing ions, claiming that the balance between attractive and repulsive forces between ions as well as the equilibrium between associated and dissociated species plays an important role in the correlation between ionic size and diffusive properties.

The linearity of D_- as a function of $1/\eta$ observed in this study can be rationalized considering that the TFSI anion is in common for the all ionic liquids and therefore does not represent a size variable (see equations (1) and (2)). The fractional form of the Stokes-Einstein equation can therefore be applied, whereby the power-law fit of our data yields a β value of 0.99795. On the other hand, equation (2) looses sense for the cations' self-diffusion data since these evidently vary in size (through the length of the alkyl side chains) and $1/r_+$ can not be assumed to be constant. In fact, the D_+ dependence on inverse viscosity hides a more complex dynamic-structure relationship.

3.3 Local structure

Figure 4 shows the diffraction patterns recorded by SAXS for the 1-alkyl-3-methylimidazolium ionic liquids, where n increases from bottom to top. Three main diffraction peaks can be distinguished in the ranges q≈2–4 nm^{-1} (peak I), q≈8.5–9 nm^{-1} (peak II) and q∼13.5 nm^{-1} (peak III). Similar diffraction features for the liquid state have previously also been observed in imidazolium ionic liquids of the $TFSI^-$, Cl^-, BF_4^- and PF_6^- anions.[8,9,23] As also mentioned in reference [25][24], peak II appears more intense in ionic liquids of the TFSI anion (compared to smaller anions like Cl^- or BF_4^-), as a result of larger electron density contrast in the X-ray scattering.

An increase of the temperature from 20 to 50°C, slightly modifies these diffraction patterns with a decrease of the absolute intensities, especially for peak I, and to a lesser extent a general shift to smaller q, *i.e.* to larger correlation lengths. This evolution is due to thermal volume expansion, while the broad bump observed between 20 and 30 nm^{-1} (Figure 4 and Figure 1 in SI) is due to inter-atomic correlations.

In analogy to previously investigated systems,[8,23] peak I is

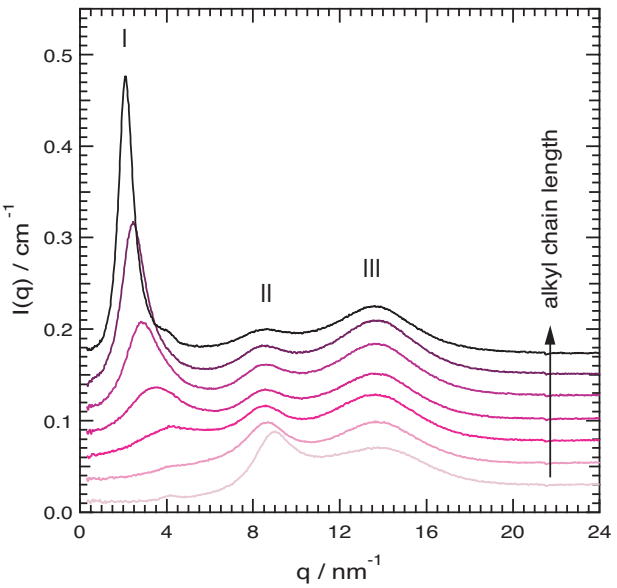

Fig. 4 X-ray scattered intensity versus scattering-vector modulus for different alkyl chain lengths at 25 °C.

** Associated to PF_6^- or $TFSI^-$.

†† Especially in $TFSI^-$ based ionic liquids compared to the BF_4^- counterparts.

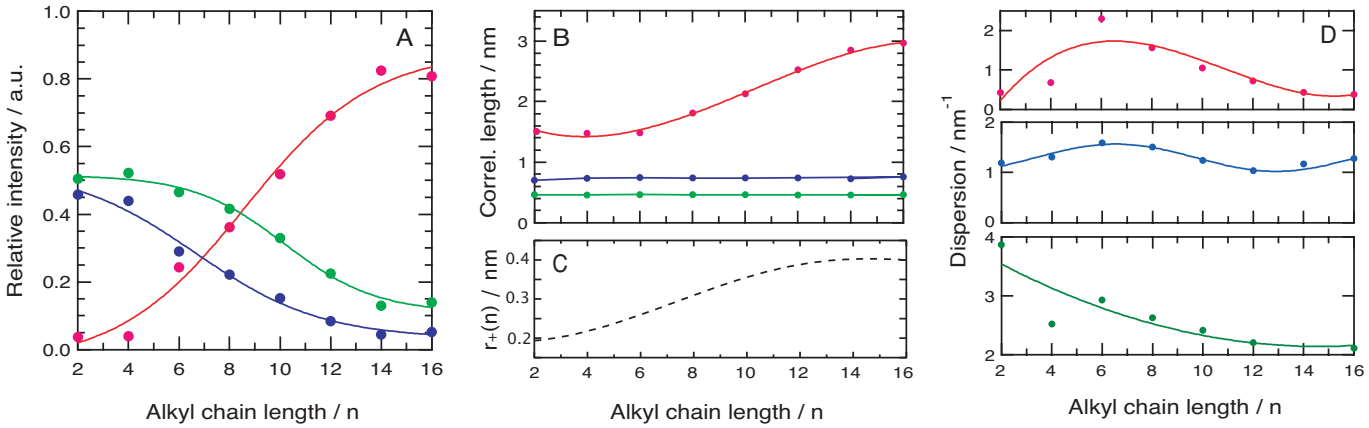

Fig. 5 A: Relative diffraction peak intensity; B: correlation lengths *d* (where d=2π/q); C: Stokes radius for the cation as a function of n extrapolated from the Stokes-Einstein relation (see eq. (3)); D: dispersion of the correlation lengths. In all graphs, data referring to peak I, peak II, and peak III are given as red, blue and green respectively. Solid lines are a guide to the eye only.

strongly dependent on the alkyl chain length and is interpreted to reflect the structural inhomogeneity in the nanometer scale occurring in ionic liquids and observed in only few other materials, like alcohols.[11] This peak clearly shifts to lower *q* values, sharpens, and gains in intensity as *n* increases. These features have been interpreted as the local structure varying from shell-to-shell, for short alkyl chains, to oily domains, for longer chains (see also reference [25][25] and the discussion therein). Peak II is characteristic for ionic liquids with large anions and can be attributed to correlations between anions, between the head group of the imidazolium ring and the anion, and between the methylene hydrogens and the anion (contributing negatively).[26] For increasing values of *n* this peak does not shift significantly in *q* and appears progressively weaker. Peak III is assigned to neighbouring shells and intramolecular correlations (as anion pair atoms, adjacent tails, cation tails with anion pairs and cation atoms)[8,27] and, similarly to peak II, does not reveal a strong dependence on *n*. Nevertheless, to get a deeper insight of these features we have employed a peak deconvolution procedure using Lorentzian functions to fit the diffraction patterns (see Figure 1 in SI). This fitting procedure allows us to analyze, beyond the peak positions, the relative intensity and the dispersion of the correlation lengths associated to the observed diffraction peaks.

The relative intensities of the three diffraction peaks are given in Figure 5A evidencing that peak I dominates the diffraction pattern for longer chain lengths, while peaks II and III become weaker. The correlation lengths, *d* (where d=2π/q), are given in Figure 5B. While *d* values for peaks II and III barely change with *n*, that of peak I (d_I) reveals a much stronger dependence. In many previous SAXS studies these cation-cation correlation lengths have been discussed to be linear with the alkyl chain length. Nevertheless, the present study reveals that this linearity strictly holds only for a limited range of *n*-values. Interestingly, in a recent paper that compares small angle neutron scattering (SANS) data on imidazolium ionic liquids of the PF_6 anion with previously reported SAXS data and MD simulations the authors propose a quadratic fit to the real space correlation lengths, which also deviates from linearity when including longer chains in the comparison.[28]

In this study, the dispersion of the correlation lengths is estimated from the HWHM (half width at half maximum) of the Lorentzian function used in the deconvolution procedure. These features have never been investigated in detail before and give us meaningful information on the local organization in ionic liquids beyond the cation-cation ordering solely. Since a dispersion curve describes the deviation from the mean of the main correlation lengths contributing towards the considered peak, it may be seen as a description of the degree of positional freedom of the different related molecular entities.

3.4 Structure - dynamic relationship

The dispersion curves for the three diffraction peaks are given in Figure 5D, and reveal different behaviors for the related main correlation lengths. While the dispersion curve of peak III monotonically decreases with n, that of peak I and II show a more complex behavior. This structural evolution suggests the existence of three distinct regimes.

For relatively short alkyl chain lengths, *i.e.* $2 \leq n \leq 6$, d_I weakly depends on *n* reflecting a negligible increase of the cationic volume. Nevertheless, the organization from an homogeneous liquid to a liquid with a nano-segregated structure results in an increased order in the non-polar domains with re-

spect to the polar ones (compare dispersion functions of peaks II and III).[29] This nascent connectivity is consistent with a high interdigitation ($\delta d/\delta n \approx 0$). Concomitant with the set in of the nano-segregation the anionic species display an increased degree of freedom (dispersion function of peak II). In fact, the growing cationic network induces a dispersive effect on the anions' average position. Despite this effect, the global decrease of the dielectric function with n[‡‡] induces a slightly higher association degree for the ion pairs thus accounting for the similar behavior of the dispersion curves for peaks II and I.

For intermediate chain lengths, *i.e.* $6 \leq n \leq 12$, d_I depends more strongly on n, and the connectivity between non-polar regions strengthens even more. Thus, this packing of the cations is consistent with the continuous decrease of the dispersion curve for peak III. In this n-range, the increase of the correlation lengths with n gives $\delta d/\delta n \approx 1.7$ Å per CH_2 unit, consistent with previous observations and indicating a weak inter-digitation of the alkyl chains.[30] In this range, both anions and cations display a decreased positional freedom, with decreasing dispersion curves. This is in agreement with the results obtained by a MD study on 1-butyl-3-methylimidazolium PF_6^- that evidenced a correlation between dynamical heterogeneity and local structure in the ionic liquid.[31] This leading effect of the cationic head on the anions' freedom is further emphasized by an overall decrease of the dielectric constant for longer alkyl chains. This trend is also consistent with the evolution of the ionicity in ionic liquids (see also Table 1 in SI).[20,32] Hence, the simultaneity of the connectivity threshold between non-polar regions and the self-diffusion coefficient inversion bridges the local structural ordering to the ionic dynamics.

For longer chain lengths, *i.e.* $n \geq 12$, the dependence of d_I on n is again weaker and $\delta d/\delta n \approx 0.6$ Å per CH_2 unit, pointing to a higher degree of inter-digitation. This relation reveals a negative deviation from strict linearity as also observed and discussed by Hardacre *et al.* in reference [28].[28] In this respect, it is worth mentioning the work by Holbrey *et al.*,[4] who have investigated the phase behavior of very long-chained 1-alkyl-3-methylimidazolium ionic liquids of the BF_4^- by detailed DSC and X-ray diffraction analysis. The authors found that for chain lengths with $n \geq 11$, the ionic liquids start to form smectic A liquid crystal phases with an enhanced local ordering. Even if the anion is different ($TFSI^-$), the trend to form such a phase is coherent with the sharpness of peak I and the stabilization of the dispersion for the related correlation distances (Figure 5D for peak I). The cations moving closer are thus packed. Nevertheless, in our systems smectic phases are formed only partially/locally, as in a sponge-like structure,[33] since the first diffraction peak shifts towards lower q values upon increased temperature (see also Figure 2 in SI).[30] For the ionic liquid with n=16, the shoulder observed close to the first diffraction peak, at $q \approx 4$ nm^{-1}, may then be attributed to (i) the second order peak of a lamellar organization since the q ratio between the first order and this eventual second order is around 1.9 and/or, (ii) defect-like structural heterogeneities in the main phases in which strong tail overlapping results in homogeneous liquid domains like those found for shorter alkyl chains. In this third region, *i.e.* $n \geq 12$, the deviation of the dispersion curve for peak II with respect to that of peak I is indicative of a weaker anion-anion ordering and consistent with the observed higher anionic diffusive constant, *i.e.* $D_- > D_+$. This can be rationalized by the stronger cation-cation correlation in the nano-segregated liquid that may leave wider volumes in the polar regions where the anions gain in motional freedom.

The behavior displayed in Figure 5B for the cation-cation correlation lengths is also compared with the Stokes radius for the cation, $r_+(n)$, derived from equation (1):

$$r_+(n) = k_B T / 4\pi D_+(n) \eta(n) \qquad (3)$$

where, assumed that $\eta(n)$ is a linear function (see inset in Figure 3C), the experimentally measured self-diffusion coefficient $D_+(n)$ is expressed as an exponential decay (from the fit of data points in Figure 3B) and a value of 4 for the coupling factor has been used, as proposed in some recent works.[12] Intriguingly, the so found Stokes radius for the cation, $r_+(n)$, displays a non-strictly linear dependence on n (see Figure 5C), consistent with the behavior of the cation-cation correlation lengths (d_I) derived from SAXS (Figure 5B). Both show that strict linearity is lost for very long chains, *i.e.* for n values ≥ 12. Although indirect, this is a further evidence for a stronger inter-digitation. Alternatively, since $r_+(n)$ reflects the size of a single cation, regardless its nano-segregated state, the weaker dependence on n for long chains may be an indication of coiling for the chain end-groups (rather than linear chain overlap as observed for n-alcohols),[10] and thus be an effect of conformational isomerism.[35] Interestingly, the Stokes radii derived from NMR data are also in very good agreement, although slightly underestimated, with the van der Waals radii calculated for ionic species in ionic liquids.[12,36] In reference 11, for instance, the van der Waals radii for the butylimidazolium (n=4) and octylimidazolium (n=8) cations are 0.303 and 0.373 nm, respectively.

To summarize, the complementary use of PFG NMR and SAXS gives new insight on the correlation between ionic dynamics and local ionic ordering. For example it could be a direct experimental probe of the coupling between conductivity relaxation time and the enthalpy relaxation time, as defined by C.A. Angell *et al.*[19] In particular, this study confirms the model of cage dynamics where the ordering of the cationic sub-network upon increased alkyl chain lengths in-

‡‡ At 25 °C, ε=12.3 for n=2, and 11.4 for n=4 in 1-alkyl-3-methylimidazolium ionic liquids of the TFSI anion.[34]

duces an overall slow down of the whole system.[37] More broadly, this study shows that the macroscopically measured transport properties in ionic liquids can be well described by a complex structuring at the nanometer scale.

4 Conclusions

By combining a large structural variation with a thorough analysis of PFG NMR and SAXS data, this study reveals new interesting correlations between transport properties and local ordering in imidazolium ionic liquids.

In particular, the self-diffusion coefficients of cations and anions have been independently measured, showing that they do not strictly follow the trend expected by the classical expression of the Stokes-Einstein relation. In fact, in contrast to what is expected from real ionic size considerations the imidazolium cations diffuse faster than the anions, up to a threshold value of n≈8, after which the opposite is observed. For long alkyl chain lengths, the higher self-diffusion coefficient of the anions is rationalized by a local structure where the strong alkyl chain connectivity slows down the cations significantly but leaves wide volumes in the polar regions in which the anions gain in motional freedom; this being a direct effect of the nano-segregation. Anions and cations also behave distinctly in that their self-diffusion coefficients show different dependences on viscosity. Moreover, the cationic hydrodynamic radius extrapolated from the Stokes-Einstein relation shows a non-strictly linear dependence on *n*, in agreement with the dependence of the cation-cation correlation lengths as found from the analysis of SAXS data. This is interpreted as a higher degree of alkyl chain inter-digitation.

New insights on the local structure in ionic liquids are also achieved from the analysis of the dispersion curves associated to the different diffraction peaks. In the regime of long alkyl chains, for instance, the dispersion of the anion-anion correlation lengths is larger than that of cation-cation, consistent with the anions diffusing faster than the cations.

5 Acknowledgments

The financial support from the Chalmers' Areas of Advance (Energy and Materials Science) are gratefully acknowledged. M.M. first acknowledges Gérard Gebel for his continuous support, Olivier Diat for his help on SAXS setup and fruitful discussions, as well as Patrick Judeinstein and Pierre Bauduin, and finally Bruno Corso and Émilie Dubard for their kind assistance on experimental measurements.

References

1 M. Freemantle, *Chem. Eng. News*, 1998, **76**(13), 32–37
2 P. Wasserscheid and T. Welton, Ionic Liquids in Synthesis, Second Edition, 2008 (eds P. Wasserscheid and T. Welton), Wiley-VCH Verlag GmbH and Co. KGaA, Weinheim, Germany
3 M. Armand, *Nature Materials*, 2009, **8**(8), 621–629
4 J.D. Holbrey, K.R. Seddon, *Journal of Chemical Society, Dalton Transactions*, 1999, **13**, 2133–2139
5 A. Martinelli et al., *Journal of Raman Spectroscopy*, 2011, **42**(3), 522-528
6 F. Gao, J. Hu, C. Peng, H. Liu, Y. Hu, *Langmuir*, 2012, **28**(5), 2950-2959
7 T. Pott, P. Méléard *Physical Chemistry Chemical Physics*, 2009, **11**(26), 5469–5475
8 A. Triolo, O. Russina, H.-J. Bleif, E. Di Cola, *Journal of Physical Chemistry B*, 2007, **111**(18), 4641–4644
9 W. Zheng, A. Mohammed, L.G. Hines Jr., D. Xiao, O.J. Martinez, R. A. Bartsch, S. L. Simon, O. Russina, A. Triolo, E. L. Quitevis, *Journal of Physical Chemistry B*, 2011, **115**(20), 6572–6584
10 A. Triolo, *Chemical Physics Letters*, 2008, **457**(18), 362–365
11 N.P. Franks, M.H. Abraham, W.R. Lieb, *Journal of Pharmaceutical Science*, 1993, **82**(5), 466–470
12 H. Tokuda, K. Hayamizu, K. Ishii, Md.A.B.H. Susan and M. Watanabe, *Journal of Physical Chemistry B*, 2005, **109**(13), 6103–6110
13 S. Tsuzuki, W. Shinoda, H. Saito, M. Mikami, H. Tokuda, M. Watanabe, *The Journal of Physical Chemistry B*, 2009, **113**(31), 10641–10649
14 H. Liu, E. Maginn, *The Journal of Chemical Physics*, 2011, **135**(12), 124507
15 A. Noda, K. Hayamizu, M. Watanabe, *Journal of Physical Chemistry B*, 2001, **105**(20), 4603–4610
16 E. O. Stejskal, J. E. Tanner, *Journal of Chemical Physics*, 1965, **42**(1), 288–292
17 R. Mills, *The Journal of Physical Chemistry*, 1973, **77**(5), 685–688
18 C.A. Angell, *Science*, 1995, **267**(5206), 1924–1935
19 C.A. Angell, *Annu. Rev. Phys. Chem.*, 1992, **43**(1), 693–717
20 H. Tokuda, S. Tsuzuki, M.A.B.H. Susan, K. Hayamizu, M. Watanabe, *Journal of Physical Chemistry B*, 2006, **110**(39), 19593-19600
21 M. Kanakubo, K.R. Harris, N. Tsuchihashi, K. Ibuki, M. Ueno, *Journal of Physical Chemistry B*, 2007, **111**(8), 2062–2069
22 A. Ahosseini, A.M. Scurto, *International Journal of Thermophysics*, 2008, **29**(4), 1222–1243
23 A. Triolo, O. Russina, B. Fazio, R. Triolo, E. Di Cola, *Chemical Physics Letters*, 2008, **457**(4-6), 362–365

24 D. Salas-de la Cruz, M.D. Green, Y. Ye, Y.A. Elabd, T.E. Long, K.I. Winey, *Journal of Polymer Science*, 2011, **50**(5), 338–346
25 W. Zheng, A. Mohammed, L.G. Hines Jr, D. Xiao, O.J. Martinez, R.A. Bartsch, S.L. Simon, O. Russina, A. Triolo, E.L. Quitevis, *Journal of Physical Chemistry B*, 2011, **115**(20), 6572–6584
26 B.L. Bhargava, R. DeVane, M.L. Klein, S. Balasubramanian, *Soft Matter*, 2007, **3**(11), 1395–1400
27 S.G. Raju, S. Bakaubramanian, *Journal of Physical Chemistry B*, 2010, **114**(19), 6455–6463
28 Hardacre, Holbrey, *The Journal of Chemical Physics*, 2010, **133**(7), 074510
29 J.N.A. Canongia, A.A.H. Padua, *Journal of Physical Chemistry B*, 2006, **110**(7), 3330–3335
30 O. Russina, A. Triolo, *Faraday Discussions*, 2012, **154**, 97–109
31 S. S. Sarangi, W. Zhao, F. Müller-Plathe and S. Balasubramanian, *ChemPhysChem*, 2010, **11**(9), 2001-2010
32 D.R. MacFarlane, M. Forsyth, E. Izgorodina, A. P. Abbott, G. Annat and K. Fraser, *Phys. Chem. Chem. Phys.*, 2009, **11**(25), 4962-4967
33 R. Atkin, G.G. Warr, *The Journal of Physical Chemistry B Letters, 2008, **112**(14), 4164-4166*
34 H. Weingartner, *Angew. Chem. Int. Ed.*, 2008, **47**(4), 654–670
35 R.Holomb, A. Martinelli, I. Albinsson, J.C. Lassègues, P. Johansson, P. Jacobsson, *Journal of Raman Spectroscopy*,2008, **39**(7), 793-805
36 M. Ue, A. Murakami, S. Nakamura, *Journal of The Electrochemical Society*, 2002, **149**(10), A1385–A1388
37 M. Kohagen, M. Brehm, Y. Lingscheid, R. Giernoth, J. Sangoro, F. Kremer, S. Naumov, C. Iacob, J. Karger, R. Valiullin, B. Kirchner, *Journal of Physical Chemistry B*, 2011, **115**(51), 15280-15288